ACS OMEGA

http://pubs.acs.org/journal/acsodf

Article

Interaction of Human Resistin with Human Islet Amyloid Polypeptide at Charged Phospholipid Membranes

Susanne Dogan,* Michael Paulus, Bastian R. Kosfeld, Christopher Cewe, and Metin Tolan

Cite This: *ACS Omega* 2022, 7, 22377−22382

Read Online

ACCESS | Metrics & More | Article Recommendations

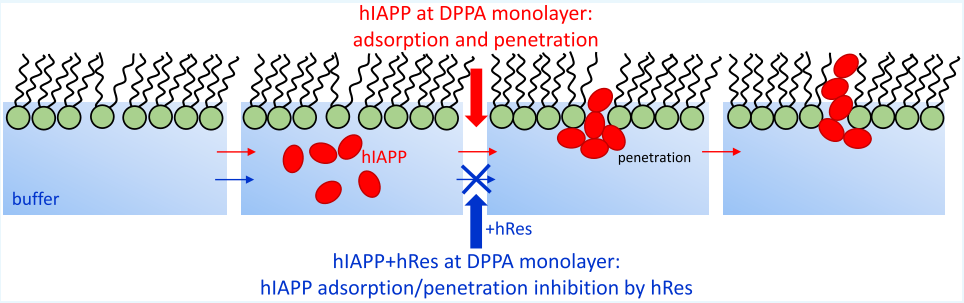

ABSTRACT: An X-ray reflectivity study on the interaction of recombinant human resistin (hRes) with fibrillation-prone human islet amyloid polypeptide (hIAPP) at anionic phospholipid Langmuir films as model membranes is presented. Aggregation and amyloid formation of hIAPP is considered the main mechanism of pancreatic β-cell loss in patients with type 2 diabetes mellitus. Resistin shows a chaperone-like ability, but also tends to form aggregates by itself. Resistin and hIAPP cross multiply metabolism pathways. In this study, we researched the potential protective effects of resistin against hIAPP-induced lipid membrane rupture. The results demonstrate that resistin can inhibit or prevent hIAPP adsorption even in the presence of aggregation-promoting negatively charged lipid interfaces. Moreover, we found strong hydrophobic interactions of resistin at the bare buffer−air interface.

INTRODUCTION

The cellular environment defines the function and structure of a protein.[1,2] Although molecular chaperones play an important role in protein folding, less is known about how they affect protein aggregation and fibrillation.

Type 2 diabetes mellitus is associated with the misfolding and aggregation of the 37-amino-acid (aa)-long peptide human islet amyloid polypeptide (hIAPP) in the Langerhans cells (β-cells) of the pancreas resulting in affecting the peripheral tissues and inhibiting insulin secretion.[3,4] The amyloid fibrils are characterized by a cross-β-sheet-rich structure, which is formed by a multistep mechanism. These can be found as amyloid plaque depositions in the pancreas of patients with type 2 diabetes mellitus.[5,6] In this context, oligomeric intermediates are classified as toxic; these can permeabilize and destroy a membrane.[7−9] Membrane interfaces, especially anionic phospholipids, can be a nucleation platform for the aggregation and subsequent plaque growth.[10−13]

Resistin is a small 108-aa-long secretory peptide (with signal sequence) expressed in adipocytes, leukocytes, macrophages, spleen, bone marrow cells, and the Langerhans cells of the pancreas.[3,4] It circulates as 92-aa peptides, which are linked by disulfide bridges in a high-(hexamer) and low-(monomer, dimer, and trimer) density form.[14] Resistin seems to act as a molecular chaperone, as it prevents the complete denaturation of enzymes by binding to the misfolded state and supports the refolding of thermally label proteins.[15] Moreover, it was shown that resistin interacts with amyloid-β (Aβ), the key molecule in the pathophysiological condition of Alzheimer's disease. Aβ and hIAPP have similar structural characteristics,[16−18] and resistin has been shown to interact with Aβ and act as a neuroprotective peptide. However, human resistin also undergoes conformational changes, which result in β-sheet structures comparable with those in pathophysiological conditions of prion proteins.[19,20] Resistin was postulated to be the missing key molecule in the relationship between obesity and diabetes.[21−23] Investigations on the polypeptide level in interaction with hIAPP are lacking. There are some studies about the inhibition of hIAPP aggregation by natural products, their derivatives,[11,24,25] and molecular crowders,[26] but there are few studies on the interaction of protein chaperones with hIAPP.[2,27,28] This paper focuses on the interaction of human resistin with human IAPP at anionic phospholipid model

Received: March 7, 2022
Accepted: May 19, 2022
Published: June 16, 2022

https://doi.org/10.1021/acsomega.2c01363
ACS Omega 2022, 7, 22377−22382

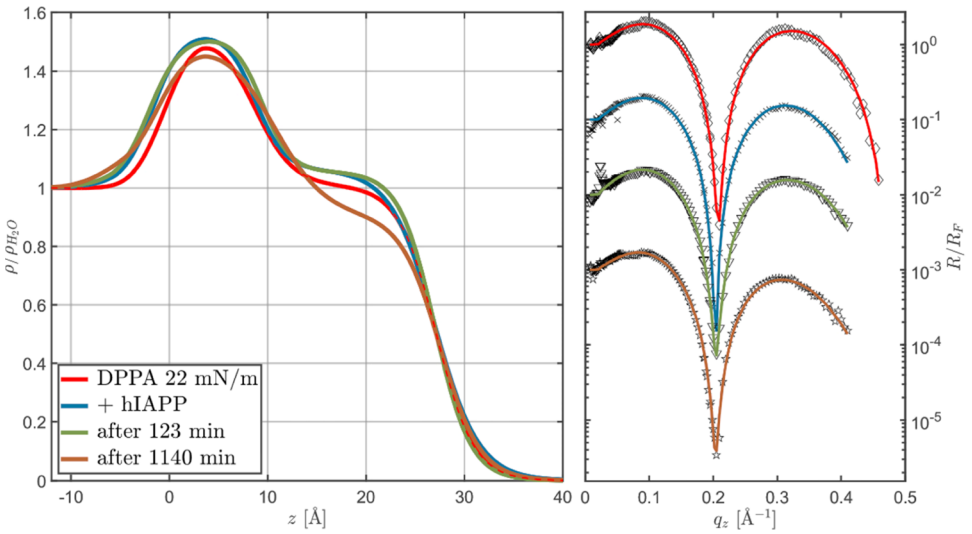

Figure 1. Normalized electron density profiles (left) and XRR data (right) of DPPA films before (red) and after the addition of hIAPP (colored). The fits are shown in the corresponding color of the electron density profile.

membranes. We show that human resistin inhibited the oligomerization of hIAPP at the membrane. This study suggests resistin as a molecular chaperone and a molecular link in cellular stress during pathological situations like type 2 diabetes mellitus and obesity.

EXPERIMENTAL SETUP

Human IAPP was purchased from Calbiochem (via Merck, Darmstadt, Germany) and human resistin (c = 1.03 mg/mL) from RayBiotech (via Hölzel-Biotech). Human IAPP was dissolved in 1,1,1,3,3,3-hexafluoro-2-propanol (c = 0.5 mg/mL) and freeze-dried in 200 μL of aliquots to break up preformed fibrils or oligomers into monomers again.[26,29] Buffer components ($Na_2HPO_4{\cdot}2H_2O$ and KH_2PO_4) and solvents (chloroform and methanol) were obtained from Merck (Darmstadt, Germany). 1,2-Dipalmitoyl-sn-glycero-3-phosphate (sodium salt, DPPA) was purchased from Avanti Polar Lipids (Alabaster, AL) and prepared as a c = 10 mg/mL solution in 9:1 chloroform/methanol. This anionic phospholipid can simulate the membrane composition in the insulin secretory granules of the pancreatic β-cell wall, since these lipids occur up to 5-fold more often than in the other cells.[30] The surface pressures were achieved by dropping appropriate amounts (50−150 μL) of the lipid solution onto the sample surface. The peptides were injected carefully underneath the Langmuir film.

The adsorption of hIAPP with c = 0.01 mg/mL (0.26 mM) and hRes with c = 0.0025 mg/mL (0.02 mM) was studied separately and in combination at the DPPA film. Four hundred microliters of Sørensen's phosphate buffer solution (pH 7) was added to 0.4 mg of lyophilized hIAPP to obtain a sample solution for the X-ray reflectivity (XRR) measurements. All prepared hIAPP solutions were used immediately after preparation. Resistin was used as it was supplied (100 μL of a 1.03 mg/mL stock solution). All mixtures were prepared in Eppendorf reaction tubes and injected carefully underneath the Langmuir film. This is performed by carefully puncturing the lipid film and injecting the solution under the film at different points. The surface pressure is a good indicator of whether the monolayer is still stable. To prevent sample volume changes, an appropriate amount of buffer was removed from the sample plate after the DPPA film reference measurement and before injecting the peptide solution. The surface pressure was set to 22 mN/m for the hIAPP measurement, and for the mixture a surface pressure of 25 mN/m was reached, mimicking the film pressure of a physiological cell membrane. Thus, the untilted liquid condensed phase of DPPA was present. In addition, hRes was examined at different surface pressures of DPPA (2.4, 23, and 44.2 mN/m) and at the bare buffer interface, which was applied as a model system for extremely hydrophobic interfaces. All measurements were conducted at room temperature and at a constant surface area.

With X-ray reflectivity, the vertical structure of Langmuir films can be determined. The reflected intensity of an X-ray beam with a defined wavelength is recorded as a function of the incidence angle α_i. In the XRR scattering geometry, the wave vector transfer $\boldsymbol{q}$ has only the vertical component $q_z = (4\pi/\lambda)\sin\alpha_i$. Laterally averaged electron density profiles $\rho_e(z)$ perpendicular to the surface can be determined from the XRR data. The XRR curves were recorded with a Bruker-AXS D8 laboratory diffractometer using copper K_α radiation with a photon energy of 8.05 keV in θ-θ geometry. Here, a typical X-ray reflectivity scan took around 1 hour. Due to the large beam size (10 × 0.1 mm^2) and the low photon flux (5 × 10^5 photons/s), no radiation damage is expected and this was also proven in control measurements.

The raw data were background corrected, intensity- and Fresnel-normalized (R/R_F), and scaled as a function of q_z. To extract information on electron density profiles, XRR curves were evaluated by a refinement of a model reflectivity curve, with a calculated initial density profile, to the real data using the combination of the Parratt algorithm and effective density model.[31,32] The simplest and appropriate model for a lipid film is a two-layer model, representing the head and tail groups. The layers are described by the parameters d (layer thickness), ρ (distinct electron density), and σ (roughness of the interface between the layers). The literature values were assigned to the roughness and electron density of the buffer subphase.[32,33] The pure lipid measurements were used as a reference to maintain the behavior of peptides at the phospholipid film.

https://doi.org/10.1021/acsomega.2c01363
ACS Omega 2022, 7, 22377−22382

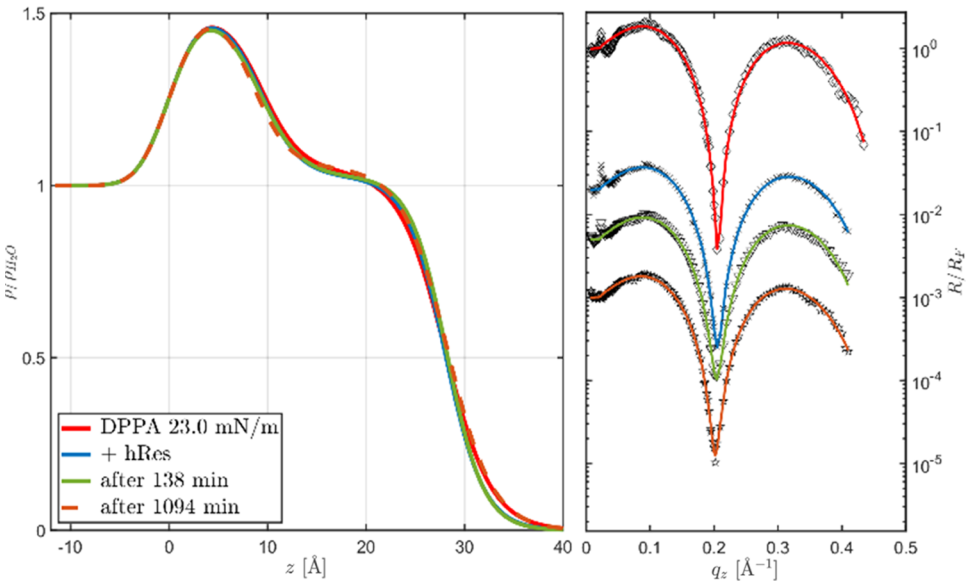

Figure 2. Normalized electron density profiles (left) and XRR data (right) of DPPA films before (red) and after the addition of human resistin (colored). The fits are shown in the corresponding color of the electron density profile.

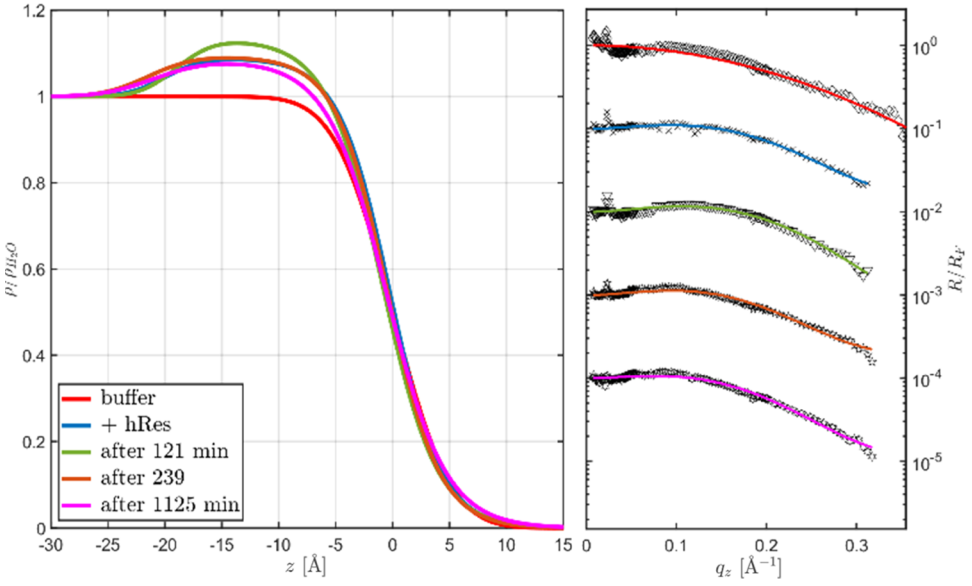

Figure 3. Normalized electron density profiles (left) and XRR data (right) of the buffer−air interface before (red) and after the addition of human resistin (colored). The fits are shown in the corresponding color of the electron density profile.

RESULTS AND DISCUSSION

Figure 1 shows the reflectivity curves and the extracted electron density profiles taken at the DPPA film before and after hIAPP was added. The density profiles indicate hIAPP-induced changes for the whole observed time range. The surface pressure increases from the initial surface pressure of 22 mN/m continuously to a saturation pressure of 31 mN/m.

The thickness of the pure DPPA layer (red) is (27.2 ± 0.15) Å, which corresponds to the nontilted liquid condensed phase. Immediately after the injection of hIAPP underneath the Langmuir film, the sample was adjusted and measured (adjustment time: ∼10 min). The change of electron density profiles over time shows the continuous increase of the layer thickness in the head group and an increase of the electron density in the head and tail groups. The head group layer thickness increases by (3 ± 0.1) Å. Since the alkyl chains of DPPA are already fully extended, no further increase in film thickness is observed, also not with hIAPP. Penetration of the peptide into the membrane causes further compression of lipids. Since the measurements were performed at a constant surface area, the electron density in the head and tail groups increases accordingly due to the penetration of hIAPP into the Langmuir film. This is also reflected in the surface pressure, which also increases.

The isoelectric point of hIAPP estimated from its amino acid sequence is 8.9.[34] hIAPP interacts with its positively charged N-terminal amino acid residues via electrostatic interaction with the anionic DPPA layer and approaches it. In the first step, this leads to the insertion into the head groups and near the hydrophobic alkyl chains, and in the next step, the entire layer is penetrated. The promotion of aggregation and fibrillation of hIAPP at an anionic lipid membrane through

https://doi.org/10.1021/acsomega.2c01363
ACS Omega 2022, 7, 22377−22382

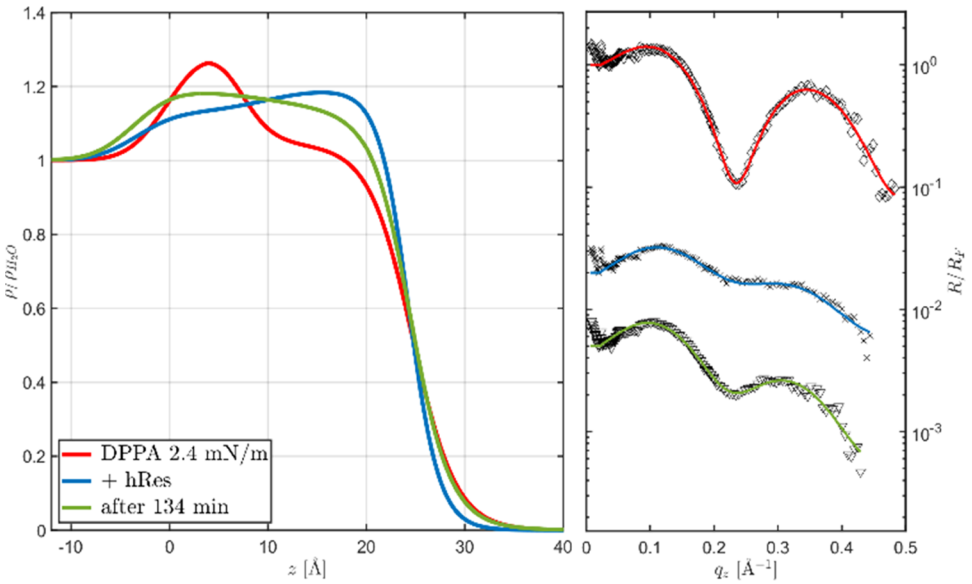

Figure 4. Normalized electron density profiles (left) and XRR data (right) of the DPPA film before (red) and after the addition of human resistin (colored). The fits are shown in the corresponding color of the electron density profile.

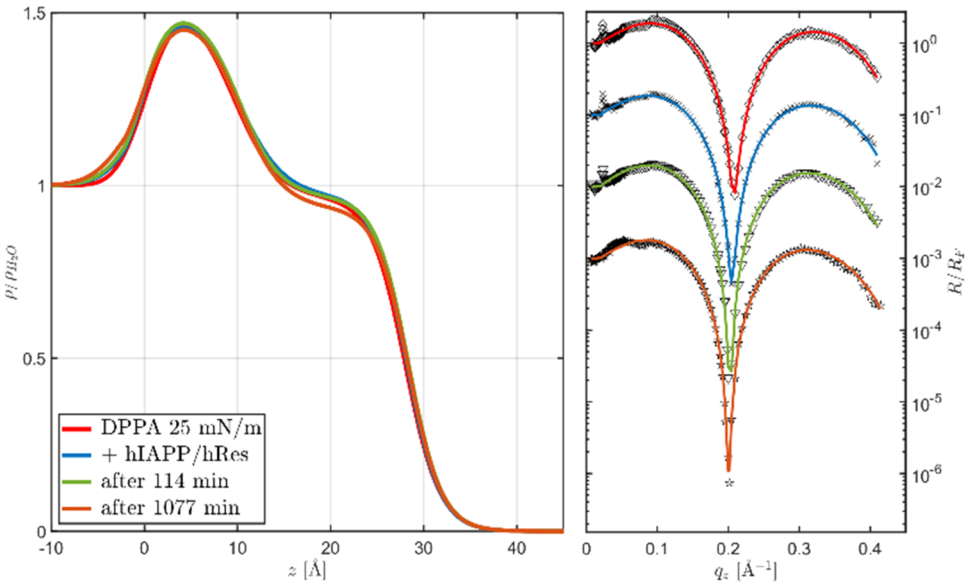

Figure 5. Normalized electron density profiles (left) and XRR data (right) of the DPPA film before (red) and after the addition of human resistin and IAPP (colored). The fits are shown in the corresponding color of the electron density profile.

the insertion of its N-terminal sequence region could already be shown.[35−38] hIAPP undergoes a multistep process of aggregation in the pathophysiological state of type 2 diabetes mellitus.[39]

The model did not improve when an additional layer was added. These are indications that hIAPP penetrates deeply into the monolayer and extends through the membrane from the buffer−head interface to the tail−air interface.

Upon further incubation of hIAPP (1140 min), the electron density decreases throughout the layer without layer thickness change, indicating that DPPA molecules and embedded pre-oligomerized hIAPP detach from the lipid phase.

Next, we studied the adsorption of human resistin at DPPA films with a different surface coverage of DPPA. In the region of the nontilted liquid expanded phase of DPPA, no effect of resistin on the film can be observed. Exemplary for the high surface pressures, the measurement at 23 mN/m is shown in Figure 2.

Resistin has no affinity for charged DPPA films. The isoelectric point of human resistin is 8.01.[40] The positive electrostatic potential in the head domain (β-strand "jelly roll" structure) is not sufficient to overcome the negative net charge.

Protein chaperones possess a high surface hydrophobicity.[41−43] Due to this fact, we investigated the adsorption of resistin at a bare buffer−air interface (Figure 3). This approach yields information about the interaction with defects in DPPA film regions at a low surface coverage (Figure 4) and helps to estimate the contribution to electron density profiles that result when hIAPP is also added.

As shown in Figure 3, resistin adsorbs at the hydrophobic buffer−air interface and forms layers ranging from (19.7 ± 0.3)

https://doi.org/10.1021/acsomega.2c01363
ACS Omega 2022, 7, 22377−22382

Å at 121 min to (21 ± 0.3) Å at 1125 min. A one-layer system was used to model the resistin film.

The protein film appears to change slightly as a function of time at the interface. The saturation pressure of 22 mN/m was confirmed in successive measurements.

As shown in Figure 4, resistin has a significant effect on the monolayer at a low surface coverage of the lipid (2.4 mN/m). This can be explained by hydrophobic interactions with the buffer−air interface, which is accessible at a lower packing density.

The restructuring of the monolayer starts immediately after the injection of hRes (blue) under the DPPA film. The surface pressure increases rapidly up to a maximum of 10.5 mN/m. The resulting total layer thickness is (27.4 ± 1) Å. It was not necessary to add an additional layer to accurately model the data. After resistin incorporation into the Langmuir film, a proper separation from the head and tail groups is no longer possible.

Finally, the interaction of hIAPP with the DPPA membrane has been examined in the presence of resistin. The electron density profiles and XRR data are displayed in Figure 5.

Compared with the single peptide measurements of human IAPP (see Figure 1) at DPPA films, different density profiles are obtained. We observed an intact and long-term stable lipid film, comparable to the measurements of resistin at the DPPA film, which showed no interaction. Resistin appears to inhibit the insertion and penetration ability of hIAPP, which may indicate its chaperone activity. Possibly, the inhibition occurs by binding to hydrophobic sites of hIAPP. However, we cannot make any statement about the conformational status of polypeptides upon interaction.

This X-ray reflectivity study addresses the interaction of hIAPP and resistin at anionic polypeptide films. In summary, we observed the adsorption and penetration of hIAPP at anionic DPPA films by an increase of the electron density and an inhibition of this effect by the addition of resistin to the system. We also observed a surface pressure dependence of the adsorption of resistin; it adsorbs via hydrophobic interactions at the water−air interface and at anionic lipid membranes with a low surface coverage.

CONCLUSIONS

In this study, we investigated the influence of human islet amyloid polypeptide and resistin separately and in combination on anionic phospholipid model membranes. First, XRR studies of hIAPP were performed at DPPA lipid interfaces in the untilted liquid condensed phase. As anionic phospholipid membranes act as nucleation centers for this amyloidogenic and fibrillation-prone peptide, adsorption could be observed within the DPPA layer. After the growth of larger structures in the lipid layer, the density profiles show a reduction in the entire lipid film, which was not observed in time-dependent measurements of pure DPPA and with resistin over a longer period of time. This suggests that the resulting hIAPP structures embed lipids and disperse them into the subphase.

Human resistin strongly interacts via hydrophobic interactions with the pure buffer−air interface yielding the formation of an adsorption layer. From the observed layer thickness, one may conclude that resistin adsorbs with the long axis in the plane of the interface. Indeed, resistin possesses no large hydrophobic core within the "head" region, which is characterized as a β-stranded sandwich (jelly roll) structure, but the tail region with its α-helical segments generates surface-exposed hydrophobicity. Resistin also has an effect on DPPA films with low surface pressures due to more accessible free buffer areas between the condensed regions; the complete monolayer is restructured by the peptide.

The measurements of human IAPP and resistin in a mixture suggest a molecular chaperone-like ability of resistin. It prevents the adsorption of hIAPP at the aggregation-fostering anionic phospholipid membrane. We suggest that resistin binds to exposed hydrophobic regions with its own hydrophobic patches and acts as a block/hindrance for further hIAPP attachment. The inhibition takes place in the early stages since no attachment to the lipid membrane was detected.

In conclusion, resistin has been the subject of numerous studies, but the literature is lacking on its interaction with amyloidogenic and fibrillation-prone peptides and its molecular chaperone ability. This study provides a hint to this specific activity and elucidates the property of resistin.

It would be useful to perform further experiments at this point, such as changing the concentration of polypeptides (hIAPP:hRes) to detect the turning point of the effect. Detection of cross-seeding of hIAPP with amyloid-β at the membrane and the effect of resistin would also be an extension of this study. Studies that allow a conformational analysis of membrane-bound or resistin-bound hIAPP, as well as resistin in bulk, would be helpful in understanding the mechanism underlying this effect.

AUTHOR INFORMATION

Corresponding Author

Susanne Dogan − *Fakultät Physik/DELTA, Technische Universität Dortmund, 44227 Dortmund, Germany;* orcid.org/0000-0003-2140-3047; Email: susanne.dogan@tu-dortmund.de

Authors

Michael Paulus − *Fakultät Physik/DELTA, Technische Universität Dortmund, 44227 Dortmund, Germany*

Bastian R. Kosfeld − *Fakultät Physik/DELTA, Technische Universität Dortmund, 44227 Dortmund, Germany*

Christopher Cewe − *Fakultät Physik/DELTA, Technische Universität Dortmund, 44227 Dortmund, Germany*

Metin Tolan − *Fakultät Physik/DELTA, Technische Universität Dortmund, 44227 Dortmund, Germany*

Complete contact information is available at: https://pubs.acs.org/10.1021/acsomega.2c01363

Author Contributions

S.D. designed the research. S.D., B.K., and C.C. performed the research. S.D. and M.P. analyzed the data. S.D. wrote the paper with the contributions of co-authors. M.T. supervised the work.

Notes

The authors declare no competing financial interest.

REFERENCES

(1) Hegyi, H.; Gerstein, M. The relationship between protein structure and function: a comprehensive survey with application to the yeast genome. *J. Mol. Biol.* **1999**, *288*, 147−164.

(2) Gao, M.; Estel, K.; Seeliger, J.; Friedrich, R. P.; Dogan, S.; Wanker, E. E. Modulation of human IAPP fibrillation: cosolutes, crowders and chaperones. *Phys. Chem. Chem. Phys.* **2015**, *17*, 8338−8348.

https://doi.org/10.1021/acsomega.2c01363
ACS Omega 2022, 7, 22377−22382

(3) Westermark, P.; Andersson, A.; Westermark, G. T. Islet amyloid polypeptide, islet amyloid, and diabetes mellitus. *Physiol. Rev.* **2011**, *91*, 795−826.
(4) Abedini, A.; Schmidt, A. M. Mechanisms of islet amyloidosis toxicity in type 2 diabetes. *FEBS Lett.* **2013**, *587*, 1119−1127.
(5) Subedi, S.; Sasidharan, S.; Nag, N.; Saudagar, P.; Tripathi, T. Amyloid Cross-Seeding: Mechanism, Implication, and Inhibition. *Molecules* **2022**, *27*, 1776.
(6) Xie, J.; Tong, Z.; Shen, L.; Shang, Y.; Li, Y.; Lu, B. Amylin: new insight into pathogenesis, diagnosis, and prognosis of non-insulin-dependent diabetes-mellitus-related cardiomyopathy. *Emerg. Crit. Care Med.* **2022**, *2*, 32−38.
(7) Brender, J. R.; Salamekh, S.; Ramamoorthy, A. Membrane Disruption and Early Events in the Aggregation of the Diabetes Related Peptide IAPP from a Molecular Perspective. *Acc. Chem. Res.* **2012**, *45*, 454−462.
(8) Weise, K.; Radovan, D.; Gohlke, A.; Opitz, N.; Winter, R. Interaction of hIAPP with model raft membranes and pancreatic beta-cells: cytotoxicity of hIAPP oligomers. *ChemBioChem* **2010**, *11*, 1280−1290.
(9) Pillay, K.; Govender, P. Amylin Uncovered: A Review on the Polypeptide Responsible for Type II Diabetes. *Biomed. Res. Int.* **2013**, *2013*, No. 826706.
(10) Lopes, D. H. J.; Meister, A.; Gohlke, A.; Hauser, A.; Blume, A.; Winter, R. Mechanism of Islet Amyloid Polypeptide Fibrillation at Lipid Interfaces Studied by Infrared Reflection Absorption Spectroscopy. *Biophys. J.* **2007**, *93*, 3132−3141.
(11) Evers, F.; Jeworrek, C.; Tiemeyer, S.; Weise, K.; Sellin, D.; Paulus, M. u. a. Elucidating the Mechanism of Lipid Membrane-Induced IAPP Fibrillogenesis and Its Inhibition by the Red Wine Compound Resveratrol: A Synchrotron X-ray Reflectivity Study. *J. Am. Chem. Soc.* **2009**, *131*, 9516−9521.
(12) Sellin, D.; Yan, L. M.; Kapurniotu, A.; Winter, R. Suppression of IAPP fibrillation at anionic lipid membranes via IAPP-derived amyloid inhibitors and insulin. *Biophys Chem.* **2010**, *150*, 73−79.
(13) Knight, J. D.; Miranker, A. D. Phospholipid catalysis of diabetic amyloid assembly. *J. Mol. Biol.* **2004**, *341*, 1175−1187.
(14) Bakry, M.; Abd El-Hameed, N. E.; Abd El-Aziz, R. M.; Hamada, M. M. Z. Resistin; a physiological overview. *Zagazig Vet. J.* **2021**, *49*, 78−91.
(15) Suragani, M.; Aadinarayana, V. D.; Pinjari, A. B.; Tanneeru, K.; Guruprasad, L.; Banerjee, S. Human resistin, a proinflammatory cytokine, shows chaperone-like activity. *Proc. Natl. Acad. Sci. U.S.A.* **2013**, *110*, 20467−20472.
(16) Hu, R.; Zhang, M.; Chen, H.; Jiang, B.; Zheng, J. Cross-Seeding Interaction between β-Amyloid and Human Islet Amyloid Polypeptide. *ACS Chem. Neurosci.* **2015**, *6*, 1759−1768.
(17) Oskarsson, M. E.; Paulsson, J. F.; Schultz, S. W.; Ingelsson, M.; Westermark, P.; Westermark, G. T. In vivo seeding and cross-seeding of localized amyloidosis: a molecular link between type 2 diabetes and Alzheimer disease. *Am. J. Pathol.* **2015**, *185*, 834−846.
(18) Raimundo, A. F.; Ferreira, S.; Martins, I. C.; Menezes, R. Islet Amyloid Polypeptide: A Partner in Crime With Aβ in the Pathology of Alzheimer's Disease. *Front. Mol. Neurosci.* **2020**, *13*, 35.
(19) Aruna, B.; Ghosh, S.; Singh, A. K.; Mande, S. C.; Srinivas, V.; Chauhan, R. Human Recombinant Resistin Protein Displays a Tendency To Aggregate by Forming Intermolecular Disulfide Linkages. *Biochemistry* **2003**, *42*, 10554−10559.
(20) Aruna, B.; Islam, A.; Ghosh, S.; Singh, A. K.; Vijayalakshmi, M.; Ahmad, F. Biophysical Analyses of Human Resistin: Oligomer Formation Suggests Novel Biological Function. *Biochemistry* **2008**, *47*, 12457−12466.
(21) Steppan, C. M.; Bailey, S. T.; Bhat, S.; Brown, E. J.; Banerjee, R. R.; Wright, CM. u. a. The hormone resistin links obesity to diabetes. *Nature* **2001**, *409*, 307−312.
(22) Flier, J. S. The missing link with obesity? *Nature* **2001**, *409*, 292−293.
(23) Ehtesham, N. Z. Molecular link between diabetes and obesity: The resistin story. *Curr. Sci.* **2001**, *80*, 1369−1371.
(24) Zelus, C.; Fox, A.; Calciano, A.; Faridian, B. S.; Nogaj, L. A.; Moffet, D. A. Myricetin inhibits islet amyloid polypeptide (IAPP) aggregation and rescues living mammalian cells from IAPP toxicity. *Open Biochem. J.* **2012**, *6*, 66.
(25) Pithadia, A.; Brender, J. R.; Fierke, C. A.; Ramamoorthy, A. Inhibition of IAPP aggregation and toxicity by natural products and derivatives. *J. Diabetes Res.* **2016**, *2016*, 1−12.
(26) Seeliger, J.; Werkmüller, A.; Winter, R. Macromolecular Crowding as a Suppressor of Human IAPP Fibril Formation and Cytotoxicity. *PloS One* **2013**, *8*, No. e69652.
(27) Martinez Pomier, K.; Ahmed, R.; Melacini, G. Interactions of intrinsically disordered proteins with the unconventional chaperone human serum albumin: From mechanisms of amyloid inhibition to therapeutic opportunities. *Biophys. Chem.* **2022**, *282*, No. 106743.
(28) Chilukoti, N.; Sil, T. B.; Sahoo, B.; Deepa, S.; Cherakara, S.; Maddheshiya, M. u. a. Hsp70 Inhibits Aggregation of IAPP by Binding to the Heterogeneous Prenucleation Oligomers. *Biophys. J.* **2021**, *120*, 476−488.
(29) Higham, C. E.; Jaikaran, E. T. A. S.; Fraser, P. E.; Gross, M.; Clark, A. Preparation of synthetic human islet amyloid polypeptide (IAPP) in a stable conformation to enable study of conversion to amyloid-like fibrils. *FEBS Lett.* **2000**, *470*, 55−60.
(30) MacDonald, M. J.; Ade, L.; Ntambi, J. M.; Ansari, I. U. H.; Stoker, S. W. Characterization of phospholipids in insulin secretory granules and mitochondria in pancreatic beta cells and their changes with glucose stimulation. *J. Biol. Chem.* **2015**, *290*, 11075−11092.
(31) Parratt, L. G. Surface Studies of Solids by Total Reflection of X-Rays. *Phys Rev.* **1954**, *95*, 359−69.
(32) Tolan, M. *X-ray Scattering from Soft-matter Thin Films: Materials Science and Basic Research*; Springer, 1999.
(33) Henke, B. L.; Gullikson, E. M.; Davis, J. C. X-Ray Interactions: Photoabsorption, Scattering, Transmission, and Reflection at E = 50-30,000 eV, Z = 1-92. *At. Data Nucl. Data Tables* **1993**, *54*, 181−342.
(34) Bjellqvist, B.; Hughes, G. J.; Pasquali, C.; Paquet, N.; Ravier, F.; Sanchez, JC. u. a. The focusing positions of polypeptides in immobilized pH gradients can be predicted from their amino acid sequences. *Electrophoresis* **1993**, *14*, 1023−1031.
(35) Khemtemourian, L.; Antoniciello, F.; Sahoo, B. R.; Decossas, M.; Lecomte, S.; Ramamoorthy, A. Investigation of the effects of two major secretory granules components, insulin and zinc, on human-IAPP amyloid aggregation and membrane damage. *Chem. Phys. Lipids* **2021**, *237*, No. 105083.
(36) Jeworrek, C.; Hollmann, O.; Steitz, R.; Winter, R.; Czeslik, C. Interaction of IAPP and insulin with model interfaces studied using neutron reflectometry. *Biophys. J.* **2009**, *96*, 1115−1123.
(37) Zhang, M.; Ren, B.; Liu, Y.; Liang, G.; Sun, Y.; Xu, L. u. a. Membrane Interactions of hIAPP Monomer and Oligomer with Lipid Membranes by Molecular Dynamics Simulations. *ACS Chem. Neurosci.* **2017**, *8*, 1789−1800.
(38) Engel, M. F. M.; Khemtémourian, L.; Kleijer, C. C.; Meeldijk, H. J. D.; Jacobs, J.; Verkleij, AJ. u. a. Membrane damage by human islet amyloid polypeptide through fibril growth at the membrane. *Proc. Natl. Acad. Sci. U.S.A.* **2008**, *105*, 6033−6038.
(39) Li, S.; Micic, M.; Orbulescu, J.; Whyte, J. D.; Leblanc, R. M. Human islet amyloid polypeptide at the air−aqueous interface: a Langmuir monolayer approach. *J. R. Soc. Interface* **2012**, *9*, 3118−3128.
(40) Patel, S. D.; Rajala, M. W.; Rossetti, L.; Scherer, P. E.; Shapiro, L. Disulfide-dependent multimeric assembly of resistin family hormones. *Science* **2004**, *304*, 1154−1158.
(41) Das, K. P.; Surewicz, W. K. Temperature-induced exposure of hydrophobic surfaces and its effect on the chaperone activity of α-crystallin. *FEBS Lett.* **1995**, *369*, 321−325.
(42) Ma, F. H.; Li, C.; Liu, Y.; Shi, L. Mimicking Molecular Chaperones to Regulate Protein Folding. *Adv. Mater.* **2020**, *32*, No. 1805945.
(43) Sučec, I.; Wang, Y.; Dakhlaoui, O.; Weinhäupl, K.; Jores, T.; Costa, D. u. a. Structural basis of client specificity in mitochondrial membrane-protein chaperones. *Sci. Adv.* **2020**, *6*, No. eabd0263.

https://doi.org/10.1021/acsomega.2c01363
ACS Omega 2022, 7, 22377−22382